Ultra-Smooth and Ultra-Strong Ion-Exchanged Glass as Substrates for Organic Electronics

Daniel Käfer, Mingqian He, Jianfeng Li, Michael S. Pambianchi, Jiangwei Feng, John C. Mauro, and Zhenan Bao**

The introduction of new substrate materials into the world of electronics has previously opened up new possibilities for novel applications and device designs. Here, the use of ion-exchanged sodium aluminosilicate (NAS) glass is presented as a new type of substrate that is not only highly damage resistant, but also allows the fabrication of high performance organic electronic devices. The smoothness of the NAS glass surface enables favorable growth of the semiconductor layer, enabling high charge carrier mobilities for typical organic semiconductors, such as pentacene or C60, and a polymer semiconductor. No degradation of the device performance is observed as a result of ion migration into the active device region, and no compromise in substrate strength due to the processing conditions is made. This work suggests the possibility of new, highly durable electronic devices on glass in large area format.

1. Introduction

Ion-exchanged glass has been widely used in portable devices, such as smartphones, tablets, media players, and also in notebooks and television screens. Its wide-spread usage in consumer electronic products with displays is due to its high strength and scratch resistance while still being very thin and possessing a smooth surface. Its hardness is a result of chemical strengthening via ion exchange of Na^+ in typical glass substrates by K^+ ions. Such substitution of larger K^+ ions into sites originally occupied by smaller Na^+ ions creates a high surface compressive stress which provides robust protection against both the propagation of existing flaws in the glass and the introduction of new flaws due to handling or impact.

So far, chemically strengthened sheet glass has been used primarily as transparent cover glass to protect the underlying electronic circuits of touch-enabled devices. It is generally not suitable as a substrate for conventional silicon-based electronics because the high temperature processing required for most inorganic devices will result in alkali diffusion which can degrade the electronic devices. The alkali diffusivity increases exponentially with temperature and becomes a significant problem for ion-exchanged glass above 300 °C.[1] Alternatively, organic electronic devices offer the unique advantage of low temperature processability, making it compatible with low cost plastic substrates, such as polyesthers with typical glass transition temperatures of around 120 °C. Even though some plastic substrates are low cost and mechanically flexible, a good encapsulation material is still needed to prevent device degradation due to moisture and oxygen diffusion through the plastic substrate. Considering that large scale patterning and processing of electronic devices on glass substrates are well-established for the liquid crystal display industry, it therefore seems that the low processing temperature required for organic electronics and the enhanced damage resistance of ion-exchanged glass is potentially a good combination for mechanically robust, large-area organic electronic devices. In this study, we demonstrate that ion-exchanged glass can serve as an outstanding substrate for organic transistors with a variety of typical organic semiconductors, enabling high performance devices that show a mechanical durability not found in traditional electronic devices.

The search for new kinds of substrates is not new in the electronics world. The standard silicon wafer substrate has significant advantages, such as smoothness and excellent availability in high quality, but it also has significant disadvantages like brittleness and lack of scalability to large dimensions (12-inch diameter is the largest Si wafer commercially available). Overcoming these problems and having truly flexible products became possible when researchers started using polymers like polystyrene (PS),[2] polyethylenenaphthalate (PEN),[3] polyethyleneterephthalate (PET),[4] or polyimide[5] as substrates in organic electronic devices where low temperature processing permits their usage. This opened up a new range of possible applications, such as flexible organic light-emitting diodes (OLEDs), flexible radio-frequency tags (RFID, a possible replacement for the optical bar code), electronic papers, or even wearable electronics.[6,7] In this study we show that the disadvantages of such polymeric devices in terms of scratch resistance and degradation/durability can be overcome using ion-exchanged

Dr. D. Käfer, Prof. Z. Bao
Department of Chemical Engineering
Stanford University
381 North South Mall, Stanford, CA 94305, USA
E-mail: dkaefer1@gmail.com; zbao@stanford.edu
Dr. M. He, Dr. J. Li, Dr. M. S. Pambianchi,
Dr. J. Feng, Dr. J. C. Mauro
Corning
Incorporated, SP-FR-6, Corning, NY14830, USA

DOI: 10.1002/adfm.201202009

sodium aluminosilicate (NAS) glass as substrate, which allows for fabrication of high performance organic thin film transistor devices with strength in excess of 1 GPa.

As a demonstration of concept, we fabricated devices using several organic semiconductors of both p- and n-type and using both small molecules and polymer semiconductors. We chose the well-known small molecule semiconductors pentacene, copper(II)-phthalocyanine, C60, and a thiophene-based polymer P2TDC17FT4,[8–10] which is deposited by spin-coating instead of thermal evaporation, thus being of more interest for future large scale production and printable active components. For the dielectric layer, our previously reported cross-linked poly(vinylphenol) (PVP) was selected as it has low leakage currents and supports favorable growth of the organic semiconductor films.[11,12] OTFTs with cross-linked PVP as gate dielectrics and the aforementioned organic semiconducting films were prepared and their electrical behavior and their morphology were characterized by *I–V* curve recording and AFM, respectively. The observed morphology is consistent with that observed previously for those semiconductors in high performance OFETs, while the favorable film morphology itself is a result of the ultra-smooth surface of the ion-exchanged glass. This is demonstrated by a comparison with devices processed in parallel using unstrengthened, regular soda lime silicate (SLS) glass slides as substrates, yielding lower performance for all OFETs.

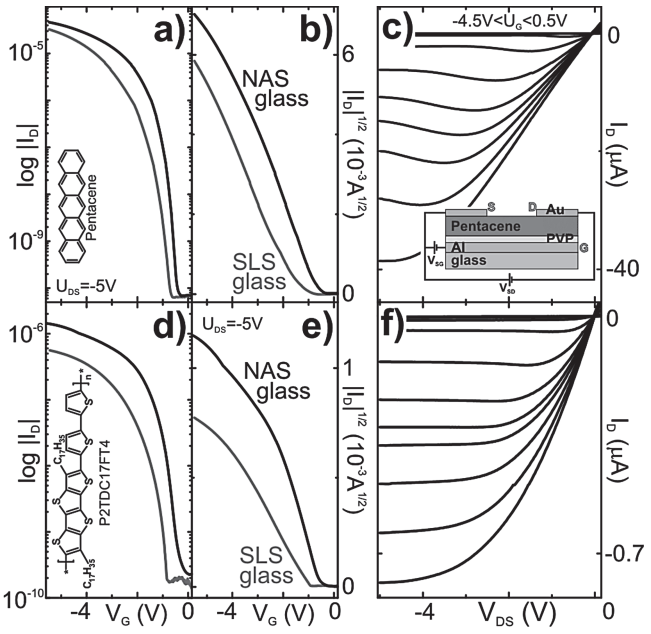

Figure 1. *I–V* characteristics of a–c) Au/50 nm pentacene/PVP/Al/ion-exchanged NAS glass OFET and for comparison also of the same device on regular SLS glass (blue curves), and d–f) of polymeric P2TDC17FT4 OFET on ion-exchanged glass and on SLS glass for comparison (blue curves). Transfer curves are shown in left part, output curves in right. The molecular structure of the active component and the principal OFET design are shown as insets in (a,d) and (c).

2. Results and Discussion

2.1. Electrical Properties

Devices on ion-exchanged glass substrates were prepared using similar procedures as previously reported. Details are described below in the experimental section. For demonstrating the versatility of ion-exchanged glass as a substrate, both p- and n-type organic semiconductors and polymers (pentacene, copper(II)-phthalocyanine, C60, and P2TDC17FT4; see **Figure 1** and **Figure 2**) have been used to prepare OFETs on it. **Table 1** summarizes the averaged numerical values obtained from the *I–V* characteristics of 12–24 devices for each semiconductor (from at least three different substrate pieces).

For pentacene thin-film OFETs the highest reported room temperature charge carrier mobility so far is μ_h = 6.4 cm^2/Vs[13] in a device using a sol-gel silica gate dielectric material. For OTS-treated SiO_2 typically maximum values of 3–4 cm^2/Vs[14,15] are reported, which is similar as what is obtained in this study. Using the polymer P2TDC17FT4, we measured a mobility of 0.19 cm^2/Vs, within the reported value of 0.33 cm^2/Vs for P2TDC13FT4[8] with shorter side chains and 0.09 cm^2/Vs for P2TDC10FT4.[9] The best electron mobility for C60 thin films is reported in the literature to be 6 cm^2/Vs[16] using hot-wall epitaxy grown (thick) films. Again the maximum values for films prepared by standard thermal evaporation are around 3 cm^2/Vs[14] and therefore also in the range obtained here. Finally, the mobility for the copper-phthalocyanine film on ion-exchanged NAS glass is also similar to those reported in the literature.[17,18]

A comparison with devices processed in parallel but on unstrengthened SLS glass slides as substrates (see blue curves in Figure 1 and Table 1) revealed that the charge carrier mobilities are superior for devices fabricated on ion-exchanged NAS glass (also true in comparison to devices prepared on PVP/Si or on SiO_2). All important parameters extracted from the *I–V* curves, such as mobility, on/off ratio and subthreshold slope, showed inferior (even though reasonable) values upon usage of unstrengthened SLS glass slides (see Table 1). The threshold voltages are also lower for the NAS glass based OFETs, which is a highly desirable feature. The low operating voltages are in general made possible by the thin PVP dielectric layer (42 nm).

A common drawback of using polymeric dielectric layers is the introduction of rather strong hysteresis of up to 10 times the voltages found in conventional SiO_2 devices due to migration of ions in the bulk polymer or at the dielectric/semiconductor interface.[6] For the devices in this study a hysteresis of 0.32/0.09/0.05/0.18 V was measured at half $I_{D,max}$ for pentacene/P2TDC17FT4/C60/CuPc devices on ion-exchanged NAS glass. Thus, with the exception of the pentacene OFET, for which also other studies have found large hysteresis on polymeric dielectrics,[19] low hysteresis was observed. A second source of hysteresis could be introduced upon usage of regular alkali-containing glass as substrate, as the highly mobile alkali ions (Na^+) can either reduce the effective hole concentration in the channel or migrate to the cathode and alter the contact, thereby causing hysteresis.[6] The thin, naturally formed, dense Al_2O_3 layer on top of the deposited Al gate electrode is known

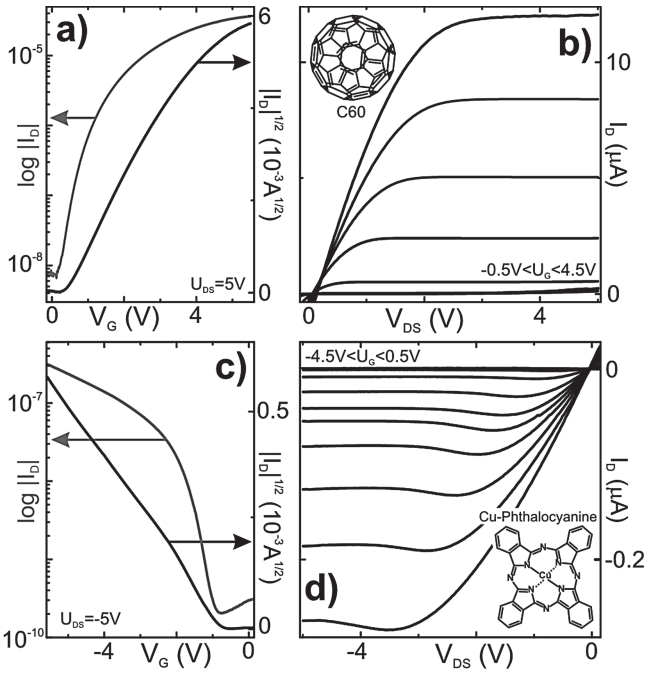

Figure 2. *I–V* characteristics of a,b) n-type C60 OFET on ion-exchanged NAS glass and c,d) CuPc OFET. Transfer and output curves are shown in (a,c) and (b,d), respectively. Molecular structures are shown as insets.

to reduce and block the ion migration[20] to some extent at least for the larger K^+ ions, but cannot completely prevent all ions from reaching the conducting channel. Identical devices made with those four organic semiconductors on PVP on Si wafers as substrate (data not shown) essentially showed the same amount of hysteresis as devices prepared on ion-exchanged glass, linking it to the dielectric layer rather than the glass substrate, which no longer contains highly mobile Na^+ ions after the ion exchange. In contrast, OFETs prepared on unstrengthened SLS glass showed higher hysteresis of 0.68/0.19/0.12/0.37 V for pentacene/P2TDC17FT4/C60/CuPc devices. This nearly doubled magnitude of hysteresis is probably caused by aforementioned mobile Na^+ ions inside the SLS glass[6] and by the increased roughness (1.43 vs 0.25 nm rms roughness for SLS vs. ion-exchanged NAS glass, see next section) and therefore

Table 1. Numerical results (averaged) of prepared OFETs on ion-exchanged NAS and regular SLS glass.

	μ [cm^2/Vs]	U_{thres} [V]	on/off	S [V/dec]
pentacene/NAS	3.82 ± 0.10	–0.78 ± 0.08	7×10^5	0.17
pentacene/SLS	2.57 ± 0.07	–1.63 ± 0.05	4×10^5	0.31
C17FT4/NAS	0.19 ± 0.02	–0.47 ± 0.08	2×10^4	0.40
C17FT4/SLS	0.08 ± 0.03	–1.00 ± 0.03	4×10^3	0.58
C60/NAS	2.53 ± 0.27	0.29 ± 0.10	6×10^3	0.98
C60/SLS	1.15 ± 0.20	0.43 ± 0.07	3×10^3	1.12
CuPc/NAS	0.028 ± 0.001	–1.82 ± 0.09	2×10^3	0.45
CuPc/SLS	0.006 ± 0.001	–2.45 ± 0.08	1×10^3	0.61

local disorder contributing to charging effects and thus also to hysteresis. The ion exchange process thus seems not only to strengthen the macroscopic material properties[21] but also the microscopic binding of the larger K^+ ions captured in the compressive stress regions[22–24] since the mobility of these species at the surface of the ion-exchanged NAS glass is dramatically reduced. In addition, annealing for several hours at 150 °C, as performed in each PVP cross-linking step, results in neither increased leakage currents nor increased hysteresis of devices on ion-exchanged NAS glass compared to those on PVP/Si substrates. There is also no change in the aforementioned device characteristics, even after two months of storage of the P2TDC17FT4 OFETs. Such stability and low hysteresis is of course highly desirable for substrates in organic electronics.

2.2. Morphology

Morphological characterizations of the fabricated OFETs were carried out and revealed a possible reason for the high performance achieved: rather large grain sizes have been formed for all semiconductor films on ion-exchanged NAS glass compared to what has been reported in literature using other substrate materials. For pentacene films terraced, pyramidal type islands of 1 to 1.5 μm size (rms roughness of (6.71 ± 0.61) nm) were observed (see **Figure 3**a), exhibiting monomolecular steps of (1.54 ± 0.05) nm height, matching the molecular length closely. Such type of morphology is typical for pentacene films on SiO_2 and also on polymers, whereas the size is rather large compared to what has been reported in literature.[25–27] In contrast, the pentacene islands on the regular SLS glass (see Figure 3b) are slightly smaller and especially their terrace size is strongly reduced. Many studies have found an increase of the charge carrier mobility with the grain size of pentacene,[2,28,29] most likely also explaining the high mobilities of OFETs on ion-exchanged glass observed in this study. In case of the polymer P2TDC17FT4 the AFM image (Figure 3c) reveals a pronounced layered terrace landscape with feature sizes of 200 nm (and step heights of 1.72 ± 0.05 nm and rms roughness of 1.50 ± 0.14 nm). This is especially interesting, since for the same polymers with shorter side chains no such distinct features and only much smaller flat domains were observed.[9,10] In general, large terraced domains are rare among polymeric semiconductor films because ordering and crystallization require more energy for polymers than for small molecules. Similar large ordered and highly crystalline terraced domains have been observed on clean SiO_2 only for the high-mobility polymer poly(2,5-bis(3-alkylthiophen-2-yl)thieno[3,2-b]thiophene (pBTTT).[30] Again the macroscopic morphology and therefore also the internal bulk crystallinity of the polymer films play a crucial role for the performance of the resulting device.[31] On SLS glass (Figure 1d) the domain size is reduced by about a third, which can thus explain the lower mobility of the device. Also for C60 films on ion-exchanged NAS glass (Figure 3e) the observed 80 nm island size is comparable to the high mobility C60 films reported in the literature.[14,32,33] The block-like compact shape (rms roughness of 6.37 ± 0.24 nm) can only be found if deposition has been performed at elevated substrate temperatures (comparable to size/shape reported in[16]) while otherwise rather featureless islands

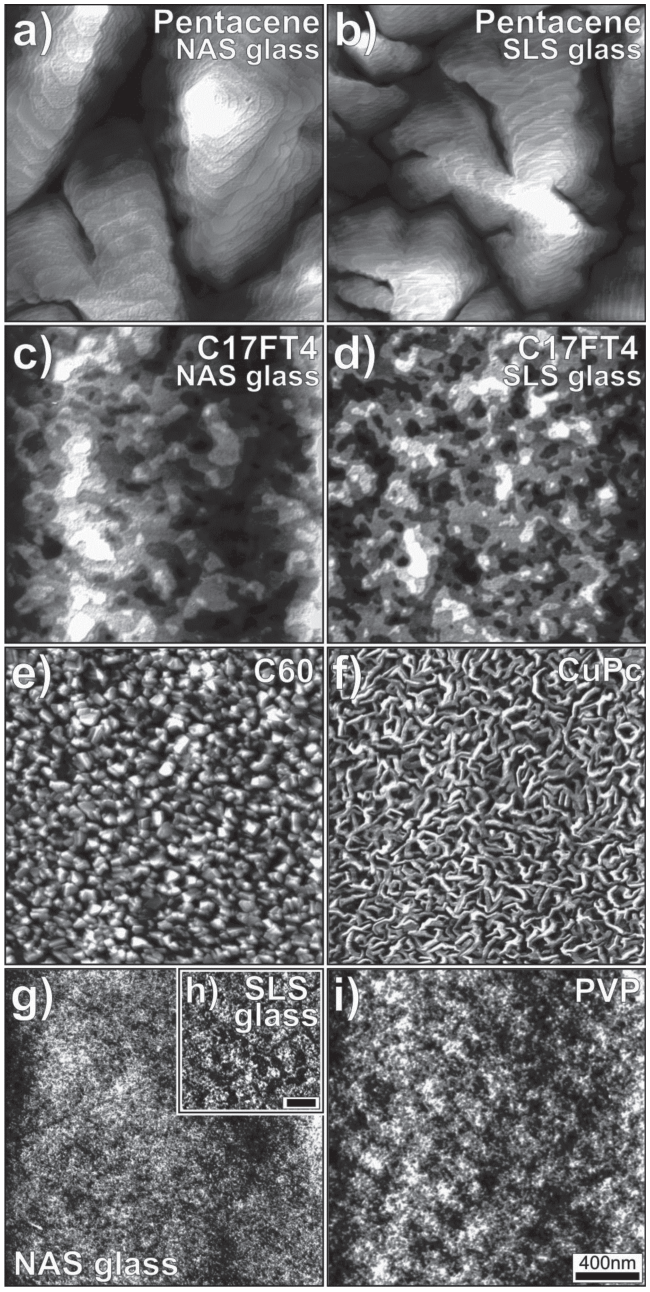

Figure 3. AFM images of 50 nm pentacene on a) PVP/Al/ion-exchanged NAS glass and on b) regular SLS glass, of 10 nm P2TDC17FT4 on c) NAS and d) SLS glass, e) of 100 nm C60 and f) 50 nm CuPc films on PVP/Al/ion-exchanged NAS glass (all inside channel region). AFM images of substrate surfaces are shown in g) for NAS, h) SLS glass, and i) PVP on NAS glass. Image size is 2 μm × 2 μm each with scale bar marking 400 nm and color palette spreading over 29/31/13/15/26/17/ 1.3/5.8/ 1.2 nm for (a–i).

result. Finally, for CuPc films up to 200-nm-long needle-like features (rms roughness of 3.88 ± 0.34 nm) can be identified on NAS glass (Figure 3f) which is similar in size (somewhat less in shape) to what has been reported in literature for films deposited at elevated temperatures.[17,34]

The larger crystalline domains seem to be consistently formed for all the semiconductors we investigated on ion-exchanged NAS glass compared to unstrengthened SLS glass substrates. A correspondingly higher mobility was also observed. Given that the device structure, materials used and fabrication process are identical on both substrates, the higher mobilities using the NAS glass are most likely due to these morphological differences. However, the question arises as to why larger domains are formed on NAS glass compared with regular SLS glass. A comparison of the AFM images of the clean substrates themselves (Figure 3g,h) showed significant differences in the overall roughness: for ion-exchanged NAS glass an rms value of 0.25 ± 0.01 nm and for SLS glass a much larger value of 1.43 ± 0.05 nm was obtained. Since the thin PVP (or BCB) dielectric layer essentially mirrors the substrate roughness, with an rms of 0.25 ± 0.01 nm for PVP/ion-exchanged glass (Figure 3i), the latter thus presented a much smoother surface to the organic semiconducting layer above. Especially for pentacene a clear correlation has been made in the literature directly linking an increased substrate roughness to decreased grain sizes[25,35,36] due to a decreased (molecular) diffusion length and reduced energy barriers for nucleation of the pentacene molecules. Furthermore, it has also been shown that the rougher the gate dielectric layer is, the lower the mobility of the resulting OFET will be because of higher defect densities probably due to an increasing number of lateral grains with (trapping) intergranular valleys in between and charge scattering caused by the rough surface.[35,37] Since the charge transport occurs primarily in the first few layers,[38] a decreased order and increase of energy barriers in those layers will almost certainly reduce the overall charge carrier mobility. It is also known that the roughness of the gate dielectrics should be below 0.25 nm because the mobility drops by a factor of 400 or more following an exponential decay as the roughness changes from 0.3 to 3 nm.[30,35,36] Interestingly, a threshold voltage shift to higher negative values has also been reported to accompany such decay.[36] Indeed, the threshold voltages for the OFETs on the rougher regular SLS glass substrate are more negative than those on the smoother fusion-drawn ion-exchanged NAS glass (cf. Table 1).

2.3. Mechanical Strength

Ion exchanged NAS glass is well known for its extraordinary high mechanical strength and scratch resistance,[1,21] even in very thin samples.[39] This is the reason why it is widely used in consumer electronic products with displays. It is especially suitable for chemical strengthening due to the strong glass network formed by the incorporation of Al_2O_3. In NAS glasses the alkali ions charge-stabilize the Al^{3+} in a tetrahedral configuration and hence strengthen the glass network, whereas in SLS glass the alkali ions tend to break bonds, forming non-bridging oxygen sites that weaken the network.[40] The mechanical strength of a chemically strengthened glass is a function of the stress profile introduced through the ion exchange process. This stress profile follows a complementary error function profile and is quantified in terms of two standard parameters: the surface compressive stress and the depth of the compressive layer. To verify that no loss of strength occurs as a result

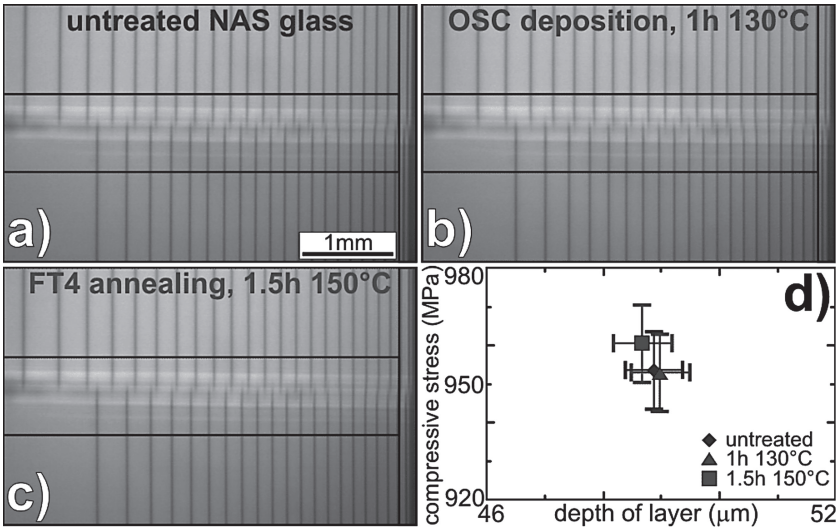

Figure 4. Optical fringe patterns obtained for a) untreated and b,c) annealed glass substrates, with samples in b) annealed 1 h at 130 °C as during OSC deposition and samples in (c) annealed 1.5 h at 150 °C as during FT4 annealing. The upper set of fringes in each image correspond to the TM mode of light propagation, and the lower fringes correspond to the TE mode. The obtained averaged values of compressive stress and depth of layer from 12 samples each together with a ±1% standard deviation are depicted in (d).

of the annealing steps required for either the OSC deposition (1 h, 130 °C) or the FT4 spin-coating (1.5 h, 150 °C) during OFET fabrication, optical fringe patterns were recorded for untreated and annealed ion-exchanged NAS glass samples (**Figure 4**a-c). The upper set of fringes in each image correspond to the TM mode of light propagation, while the lower fringes correspond to the TE mode. The offset in position between the first TM and TE fringes gives the bifringence, which, when multiplied by the stress-optic coefficient, yields the surface compressive stress of the glass. The depth of the compressive layer, on the other hand, is calculated from the number of fringes and width of the fringe pattern based on the TM mode data. The absolute values of the surface compressive stress measured are close to 1 GPa (see Figure 4d) and prove the extraordinary mechanical strength of NAS glass. Comparing the untreated and annealed samples, effectively identical optical fringe patterns are recorded and therefore also identical surface compressive stress and depth of layer values are obtained (within given error). This proves that the annealing process involved in OFET fabrication does not diminish the high strength of the ion-exchanged NAS glass. The low temperature processing used for organic electronic devices thus prevents significant stress relaxation or alkali migration in the ion-exchanged glass making ion-exchanged NAS glass perfectly suited to be used to fabricate OFETs with a mechanical durability not found in traditional electronic devices.

3. Conclusions

In summary, we have shown that the ion-exchanged NAS glass allows fabrication of high performance organic electronic devices from a wide variety of organic semiconductors (p-type, n-type, small molecules, polymers) using it as a substrate that possesses exceptional mechanical durability. The devices on ion-exchanged NAS glass showed higher electrical performance and are free of mobile ions at the glass surface, which make it a superior substrate compared to regular SLS glass substrates. The enhancing feature arises from the much smoother surface of the fusion-drawn ion-exchanged glass allowing an enhanced diffusion length and lower energy barriers for organic molecules deposited on top and yielding an improved growth of the organic semiconductor with larger grain and island sizes, fewer defects, and higher local order. This in turn maximizes the charge carrier mobility of the whole device. Furthermore, no evidence of ion migration into the active region of the devices was found, and no reduction in strength of the ion-exchanged NAS glass occurred during and after fabrication of the OFETs. Therefore, chemically strengthened NAS glass combines many advantages highly desirable for production of stable, strong, and high performing organic electronic devices.

4. Experimental Section

Top-contact OFETs were prepared on fusion-drawn ion-exchanged sodium aluminosilicate (NAS) glass, that is chemically strengthened via an ion exchange process in which Na^+ in the glass are replaced by larger K^+ ions by immersion in a bath of molten KNO_3. For comparison, OFETs were also prepared on unstrengthened, regular soda lime silicate (SLS) microscope glass slides (both types of glass were 1 mm thick and provided by Corning Incorporated). The substrates were first cleaned with soap, rinsed with DI water, toluene, acetone, and isopropanol, and ozone cleaned for 5 min. A 100-nm Al gate electrode layer was then deposited in a custom-built high-vacuum deposition system (thermionics lab, Inc.) at a rate of 13 nm/min as monitored by a quartz crystal microbalance. Polymeric dielectric layers were formed on top by spin-coating a filtered 1:10-3:1 mixture of a 40 mg/mL solution of a) PVP (poly(4-vinylphenol), Sigma-Aldrich, $M_W \approx 25\ 000$ g mol^{-1}) in PGMEA (propylene glycol monomethyl ether acetate, Sigma-Aldrich, 99.5%), b) a 1 μL/mL solution of the base triethylamine (Sigma-Aldrich, 99%, catalyst) in PGMEA, and c) a 4 mg/mL solution of HDA (4,4′-(hexafluoro-isopropylidene) diphthalic anhydride, Sigma-Aldrich, 99%) in PGMEA (60 s at 7000 rpm after 25 s delay). The layer was cross-linked by thermal annealing at 100 °C in air for 2 h before a second layer was spin-coated and annealed again (d = 42 nm). The capacitance of each substrate was measured using an "Agilent E4980A Precision LCR Meter" (≈100 nF/cm^2). For C60 devices a thin OH-group-shielding BCB (benzocyclobutene) layer was added by spin-coating and step-wise annealing (30 min at 120 °C, 20 min at 180 °C, 30 min at 240 °C). The small molecule organic semiconductors pentacene ($C_{22}H_{14}$, triple-sublimed, Sigma-Aldrich), Copper(II)-phthalocyanine (CuPc, $C_{32}H_{16}CuN_8$, Sigma-Aldrich, 99%), and the fullerene C60 (Sigma-Aldrich, 99.9%) were deposited via organic molecular beam deposition (Åmod PVD Vacuum Coating Systems, angstrom engineering) from a resistively heated quartz crucible under HV conditions at a deposition rate of 6.0/ 2.6/ 2.9 nm/min (QCM) at substrate temperatures of 333/ 371/ 403 K yielding 50/ 50/ 100 nm films of Pc/ CuPc/ C60, respectively. A further 30-min post-annealing step was added in vacuum at those temperatures. The polymeric organic semiconductor P2TDC17FT4 (Corning Inc., $M_W \approx 14\ 000$ g mol^{-1}), on the other hand, was prepared by spin-coating a filtered solution

(2 mg/mL, dichlorobenzene) of the polymer at 1500 rpm for 60 s (in glove box, after 60 s delay) and annealing in N_2 atmosphere at 150 °C for 1.5 h (d = 10 nm). For pentacene, CuPc and P2TDC17FT4 devices top electrodes with channel length dimensions of L = 50 µm and W/L = 20 were created by thermal evaporation of 40 nm Au through shadow masks at a rate of 3 nm/min under HV conditions. For C60 devices a 0.6 nm thin LiF blocking layer was deposited at a rate of 1.5 nm/min before the 50 nm Al top electrodes were prepared at a rate of 13 nm/min. All p-type TFT measurements were performed in ambient atmosphere (293 K, relative humidity 49%) using a "Keithley 4200-SCS" semiconductor parameter analyzer and standard Au wire probes, while the n-type C60 OFET was measured inside a glove box. 12 to 24 different devices from at least 3 different substrate pieces were prepared for each semiconductor and measured in each case; the average numerical values and errors are reported in table 1.

AFM was performed using a "Digital Instruments Multimode Nanoscope III" operated under ambient conditions and exclusively in tapping mode. A standard FSM-6000 optical instrument was used to measure the compressive stress and the depth of the compressive layer of untreated and differently annealed (1 h at 130 °C, 1.5 h at 150 °C) ion-exchanged NAS glass samples. Four measurements were taken on each sample, while 3 samples were used for each of the 3 cases.

Acknowledgements

D.K. acknowledges postdoctoral fellowship support from the Deutsche Forschungsgemeinschaft (DFG, German Science Foundation) through grant KA 3180/1-1.

Received: July 18, 2012
Published online: January 22, 2013

[1] M. M. Smedskjaer, Q. Zheng, J. C. Mauro, M. Potuzak, S. Morup, Y. Yue, *J. Non-Cryst. Solids* **2011**, *357*, 3744.
[2] C. Kim, A. Facchetti, T. J. Marks, *Adv. Mater.* **2007**, *19*, 2561.
[3] Y. Kato, S. Iba, R. Teramoto, T. Sekitani, T. Someya, H. Kawaguchi, T. Sakurai, *Appl. Phys. Lett.* **2004**, *84*, 3789.
[4] Y.-L. Loo, T. Someya, K. W. Baldwin, Z. Bao, P. Ho, A. Dodabalapur, H. E. Katz, J. A. Rogers, *Proc. Natl. Acad. Sci. USA* **2002**, *99*, 10252.
[5] Z. Bao, Y. Feng, A. Dodabalapur, V. R. Raju, A. J. Lovinger, *Chem. Mater.* **1997**, *9*, 1299.
[6] H. Klauk, in *Organic Electronics - Materials, Manufacturing, and Applications*, Wiley-VCH, Weinheim, Germany **2006**.
[7] Z. Bao, J. Locklin, in *Organic Field-Effect Transistors*, 1st ed., CRC, Boca Raton, FL **2007**.
[8] H. H. Fong, V. A. Pozdin, A. Amassian, G. G. Malliaras, D.-M. Smilgies, M. He, S. Gasper, F. Zhang, M. Sorensen, *J. Am. Chem. Soc.* **2008**, *130*, 13202.
[9] M. He, J. Li, M. L. Sorensen, F. Zhang, R. R. Hancock, H. H. Fong, V. A. Pozdin, D.-M. Smilgies, G. G. Malliaras, *J. Am. Chem. Soc.* **2009**, *131*, 11930.
[10] M. He, J. Li, A. Tandia, M. Sorensen, F. Zhang, H. H. Fong, V.A. Pozdin, D.-M. Smilgies, G. G. Malliaras, *Chem. Mater.* **2010**, *22*, 2770.
[11] M. E. Roberts, S. C. B. Mannsfeld, N. Queraltó, C. Reese, J. Locklin, W. Knoll, Z. Bao, *Proc. Natl. Acad. Sci. USA* **2008**, *105*, 12134.
[12] M. E. Roberts, N. Queraltó, S. C. B. Mannsfeld, B. N. Reinecke, W. Knoll, Z. Bao, *Chem. Mater.* **2009**, *21*, 2292.
[13] H. S. Tan, N. Mathews, T. Cahyadi, F. R. Zhu, S. G. Mhaisalkar, *Appl. Phys. Lett.* **2009**, *94*, 263303.
[14] Y. Ito, A. A. Virkar, S. Mannsfeld, J. H. Oh, M. Toney, J. Locklin, Z. Bao, *J. Am. Chem. Soc.* **2009**, *131*, 9396.
[15] A. Virkar, S. Mannsfeld, J. H. Oh, M. F. Toney, Y. H. Tan, G. Y. Liu, J. C. Scott, R. Miller, Z. Bao, *Adv. Funct. Mater.* **2009**, *19*, 1962.
[16] T. B. Singh, N. S. Sariciftci, H. Yang, L. Yang, B. Plochberger, H. Sitter, *Appl. Phys. Lett.* **2007**, *90*, 213512.
[17] Z. Bao, A. J. Lovinger, A. Dodabalapur, *Appl. Phys. Lett.* **1996**, *69*, 3066.
[18] J. Zhang, H. Wang, X. Yan, J. Wang, J. Shi, D. Yan, *Adv. Mater.* **2005**, *17*, 1191.
[19] S. C. Lim, S. H. Kim, J. B. Koo, J. H. Lee, C. H. Ku, Y. S. Yang, T. Zyung, *Appl. Phys. Lett.* **2007**, *90*, 173512.
[20] L. K. Cornelius, A. J. Ellison, S. Likitvanichkul, US patent, US2005/0079288A1, **2005**.
[21] K. L. Barefoot, M. J. Dejneka, S. Gomez, T. M. Gross, N. Shashidbar, US patent, US2011/0201490A1, **2011**.
[22] D. W. Rinehart, N. Heights, US patent, 3357876, **1967**.
[23] A. Y. Sane, A. R. Cooper, *J. Am. Cer. Soc.* **1987**, *70*, 86.
[24] J. E. Davidson, M. D. Ingram, A. Bunde, K. Funke, *J. Non-Cryst. Sol.* **1996**, *203*, 246.
[25] D. Knipp, R. A. Street, A. Völkel, J. Ho, *J. Appl. Phys.* **2003**, *93*, 347.
[26] S. Verlaak, S. Steudel, P. Heremans, D. Janssen, M. S. Deleuze, *Phys. Rev. B* **2003**, *68*, 195409.
[27] R. Ruiz, A. C. Mayer, G. G. Malliaras, B. Nickel, G. Scoles, A. Kazimirov, H. Kim, R. L. Headrick, Z. Islam, *Appl. Phys. Lett.* **2004**, *85*, 4926.
[28] A. Di Carlo, F. Piacenza, A. Bolognesi, B. Stadlober, H. Maresch, *Appl. Phys. Lett.* **2005**, *86*, 263501.
[29] B. Bräuer, R. Kukreja, A. Virkar, H. B. Akkerman, A. Fognini, T. Tyliszczak, Z. Bao, *Org. Electron.* **2011**, *12*, 1936.
[30] Y. Jung, R. J. Kline, D. A. Fischer, E. K. Lin, M. Heeney, I. McCulloch, D. M. DeLongchamp, *Adv. Funct. Mater.* **2008**, *18*, 742.
[31] H. N. Tsao, D. Cho, J. W. Andreasen, A. Rouhanipour, D. W. Breiby, W. Pisula, K. Müllen, *Adv. Mater.* **2009**, *21*, 209.
[32] T. D. Anthopoulos, B. Singh, N. Marjanovic, N. S. Sariciftci, A. M. Ramil, H. Sitter, M. Cölle, D. M. de Leeuw, *Appl. Phys. Lett.* **2006**, *89*, 213504.
[33] S. Kobayashi, T. Takenobu, S. Mori, A. Fujiwara, Y. Iwasa, *Appl. Phys. Lett.* **2003**, *82*, 4581.
[34] M. Krzywiecki, L. Grządziel, J. Bodzenta, J. Szuber, *Thin Solid Films* **2012**, *520*, 3965.
[35] S. Steudel, S. De Vusser, S. De Jonge, D. Janssen, S. Verlaak, J. Genoe, P. Heremans, *Appl. Phys. Lett.* **2004**, *85*, 4400.
[36] K. Suemori, S. Uemura, M. Yoshida, S. Hoshino, N. Takada, T. Kodzasa, T. Kamata, *Appl. Phys. Lett.* **2008**, *93*, 033308.
[37] D. Knipp, R. A. Street, A. R. Völkel, *Appl. Phys. Lett.* **2003**, *82*, 3907.
[38] M. Kiguchi, M. Nakayama, T. Shimada, K. Saiki, *Phys. Rev. B* **2005**, *71*, 035332.
[39] http://ceramics.org/ceramictechtoday/2012/04/19/corning-demonstrates-glass-strength-testing-methods-with-gorilla-glass/(accessed January 2013).
[40] Q. Zheng, M. Potuzak, J. C. Mauro, M. M. Smedskjaer, R. E. Youngman, Y. Yue, *J. Non-Cryst. Solids* **2012**, *358*, 993.